Symmetry Breaking in a Model for Nodal Cilia

Charles J. Brokaw

Division of Biology, California Institute of Technology
Pasadena, CA 91125, USA

Abstract. Nodal cilia are very short cilia found in the embryonic node on the ventral surface of early mammalian embryos. They create a right to left fluid flow that is responsible for determining the normal asymmetry of the internal organs of the mammalian body. To do this, the distal end of the cilium must circle in a counterclockwise sense. Computer simulations with 3-dimensional models of flagella allow examination of 3-dimensional movements such as those of nodal cilia. 3-dimensional circling motions of short cilia can be achieved with velocity controlled models, in which dynein activity is regulated by sliding velocity. If dyneins on one outer doublet are controlled by the sliding velocity experienced by that doublet, the system is symmetric, and the 3-dimensional models can show either clockwise or counterclockwise circling. My computer simulations have examined two possible symmetry breaking mechanisms: 1) dyneins on doublet N are regulated by a mixture of the sliding velocities experienced by doublets N and N+1 (numbered in a clockwise direction, looking from the base). or 2) symmetry is broken by an off-axis force that produces a right-handed twist of the axoneme, consistent with observations that some dyneins can rotate their substrate microtubules in a clockwise direction.

INTRODUCTION: THE BIOLOGY OF NODAL CILIA

About one in ten thousand humans have the condition known as situs inversus, in which the asymmetry of the internal body organs is reversed [reviewed in 1]. This condition has been known for many years, and is found in other mammals besides humans. It results from a failure of a normal developmental mechanism that solves a fundamental problem in developmental biology: How is the symmetry of the fertilized egg broken, to generate, in almost all cases, a consistent asymmetry of the internal body organs?

By itself, situs inversus usually causes no health problems, and may be undetected for years. However, situs inversus is sometimes associated with significant medical problems. This association, now recognized as “Kartagener-Afzelius syndrome” [2], has been the key to understanding situs inversus and the development of normal body asymmetry. Neither Kartagener nor Afzelius set out to study situs inversus. Manes Kartagener was an MD working in Zurich, Switzerland. He was apparently the first to study the inheritance of the combination of bronchial and sinus infections and situs inversus, and he recognized that situs inversus was not found in all of the family members who inherited the high incidence of respiratory infections. Bjorn Afzelius is a Swedish electron microscopist. Beginning in the 1950s, he was one of the earliest electron microscopists to study the microscopic anatomy of cilia and flagella. In the early 1970s, he was asked to look at the flagella of non-motile spermatozoa from some infertile men. It turned out that some of these men not only had defective sperm

CP755, *ISIS: International Symposium on Interdisciplinary Science*
edited by A. Ludu, N.R. Hutchings and D.R. Fry

flagella, but also the symptoms recognized by Kartagener. Afzelius made the connection with defective cilia in the respiratory tract, and confirmed this with electron microscopy. Afzelius speculated that cilia in the early embryo might produce a rotational movement responsible for normal asymmetry. It followed from this that if these embryonic cilia were non-motile, the asymmetry might be determined randomly, explaining a 50% incidence of situs inversus in these individuals with defective cilia.

Confirmation of Afzelius's speculation has come only in the last few years, from observations on mouse embryos. A mouse mutant with situs inversus was known since 1959 [3], and Supp et al. [4,5] reported that it resulted from a mutation in a dynein. Dyneins are the motor enzymes responsible for the movement of cilia and flagella. The laboratory of Nobutaka Hirokawa, at the University of Tokyo, was studying a kinesin, a member of the other group of motor enzymes that move along microtubules. This kinesin is essential for the assembly of cilia, and a mutant mouse defective in this kinesin has serious developmental defects. Using mutant and normal mice, Hirokawa's group was able to show that cilia in the embryonic node on the ventral surface of the mouse embryo are motile, and produce a leftward-directed fluid flow that is essential for development of proper asymmetry [6,7,8]. This flow is produced by a circling motion of these nodal cilia, which is clockwise when looking at the surface of the embryo. However, in the cilia and flagella field, it is conventional to look at cilia from base to tip, and the circling movement of nodal cilia is therefore counterclockwise in this context.

A leftward-directed fluid flow could be produced by counterclockwise circling of nodal cilia if they are, on average, tilted towards the posterior end of the embryo (which has already been determined by the critical time for left-right asymmetry appearance). When tilted posteriorly, the cilium will be moving from left to right when it is closest to the surface of the epithelium, and generation of rightward-directed fluid flow will be retarded by the surface. The cilium will be moving from right to left when it is farthest from the surface, where generation of leftward-directed flow is most effective [9]. However, the fluid movement in the nodal depression is unlikely to be this simple [10]. The sequence of steps by which a leftward-directed flow induces the development of normal asymmetry is still under active investigation, and contains multiple events that could fail and cause situs inversus that is unrelated to ciliary motility. However, the focus of the remainder of this article will be ciliary motility; specifically, what is the initial symmetry-breaking factor that causes the circling movement of nodal cilia to be counterclockwise?

Nodal cilia are very small, and difficult to see by ordinary light microscopy, so no detailed description of their bending is available. Scanning electron microscopy shows that they are only 2 or 3 μm long [11]. Transmission electron microscopy of cross-sections of nodal cilia shows the absence of the central pair of microtubules found in most motile cilia and flagella [8]. In most cases, the central pair of microtubules is required for planar bending, and three-dimensional or helical movements are found when the central pair is absent.

The cytoskeleton of cilia and flagella is known as an axoneme. The structure of the axoneme, as revealed by electron microscopy of transverse sections, is asymmetric. The dynein motor enzymes are located in the "arms" located on the A tubule of each of the 9 outer doublets (Fig. 1).

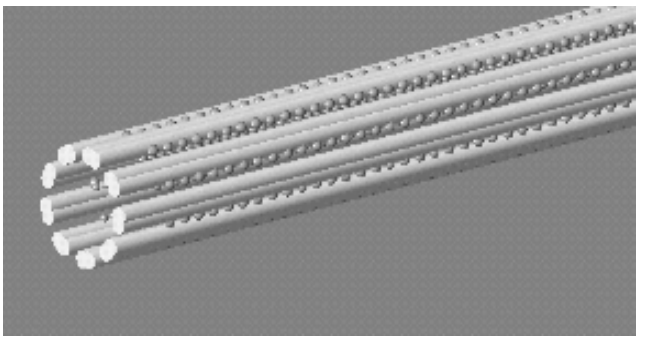

FIGURE 1. Basic elements of an axoneme, the common cytoskeleton of cilia and flagella. Nine outer microtubular doublets are arranged to form the surface of a cylinder. Dynein motor enzymes, represented here as spheres, are lined up in two rows on the A-tubule of each doublet, and produce sliding movements by interacting with the B-tubule of the adjacent doublet.

These arms are attached stably to the A tubule of the doublet, and reach around in a clockwise direction to interact with the B tubule of the adjacent doublet. This interaction produces sliding displacements between adjacent doublets [12]. In spite of the universal asymmetry of this structure, flagella from some organisms produce bending patterns that require clockwise progression of activity around the circumference of the axoneme, and flagella from other organisms require counterclockwise progression of activity. So asymmetry of function is not explained in a simple manner by asymmetry of structure. My approach to this problem is to construct a computer model of a nodal cilium and ask what features need to be incorporated into the model to obtain consistent counterclockwise circling movements.

COMPUTER MODELLING OF THREE-DIMENSIONAL MOVEMENT OF FLAGELLA AND CILIA

Three-dimensional modelling of flagella has been described in detail [13] and modified for modelling short flagella and cilia such as nodal cilia [14]. The models start by arranging the 9 outer doublets uniformly on the surface of a cylinder, as in Fig. 1, and then the doublets are just represented by parallel lines on the surface. There must be important connections and forces that are involved in maintaining this arrangement, but these are not considered in my modelling. The only distortion that is allowed is sliding (shear) between adjacent doublets; when this shear is not uniform along the length, the model must bend. Sliding between doublets is required to be 0 at the basal end of the model.

When an axoneme is bent, it acts as an elastic structure, and tries to return to a straight configuration. In other words, it has an elastic bending resistance. There are reasonably good quantitative estimates of this resistance, which have led to use of a value of 2×10^8 pN nm^2 for modelling flagella such as sea urchin sperm flagella [15]. Flagella probably also have elastic shear resistances, and they operate in a viscous

environment that resists the bending movements. These resistances are important, but they are not essential components of a computer model [16].

For numerical analysis of axonemal bending, the length of the axoneme is divided up into straight segments of equal length, with bending occuring at the joints between these segments. The rate of bending at each joint is obtained by solving a set of equations that balances the active and resistive bending moments, and these rates of bending can then be used to calculate the shape of the model as a function of time [13, 17].

Bending of the axoneme results from shear forces generated by dynein motor enzymes that are distributed uniformly along the length of each outer doublet (Fig. 1). Although no specific information about the spacing and number of dyneins in nodal cilia is available, information from other flagella has been extrapolated for this modelling. A typical flagellum appears to contain at least 9 different dyneins, with some functional differences between these dyneins. There is only very limited knowledge about how these functional differences might be significant for flagellar function [18], and for the present work they are ignored. If all of the dyneins are always producing active shear forces, they will antagonize each other, and no bending will result. So the usual assumption has been that there must be some form of local control mechanism that turns dynein activity on and off. There is no direct experimental evidence that dyneins can be turned on and off -- it has just been considered to be necessary to get a cilium or flagellum to produce bending. Most computer modelling of flagella and cilia has utilized feedback from bending to control dynein activity; these models can be referred to as “curvature controlled models” [13, 17, 19, 20].

Compared with understanding of the other motor enyzmes, myosin and kinesin, knowledge of dynein function is very limited. Dynein may operate in the manner suggested by Huxley [21] for myosin, by attaching to its substrate microtubule while it releases strain by executing a power stroke [22], and then recovering strain energy while detached from the substrate and hydrolyzing ATP [reviewed in 23]. However, dynein is significantly different and more complex that the other motor enzymes [24]. At present, we do not understand this complexity enough to introduce it into computer simulations, and the models used for dynein are basically just myosin models dressed up to look like dynein. For modelling cilia and flagella, two approaches are possible. One approach computes the force by stochastically modelling the chemical kinetics of each individual motor enzyme [13, 25]. The other approach simply calculates the active shear force generated on each doublet for each segment of the model from a simple mathematical model for a force generator. Since the stochastic modelling is computationally more demanding and requires more estimates of unknown parameters, both approaches are useful.

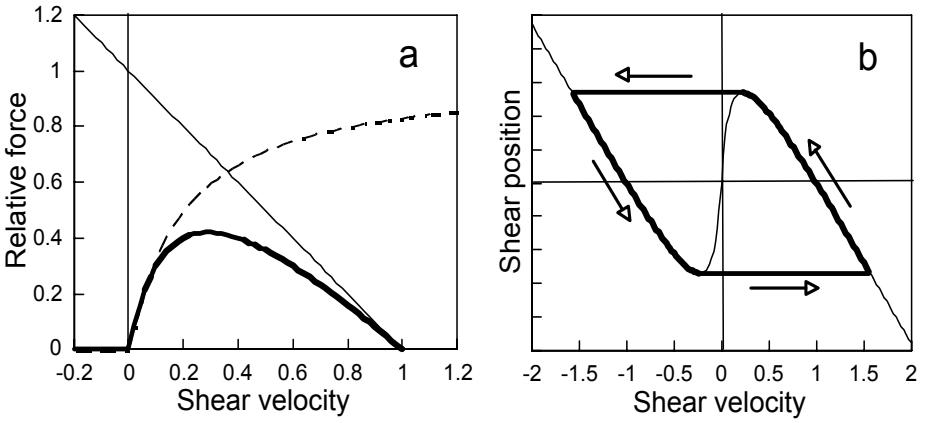

FIGURE 2. Steady-state behavior of a simple model for shear force generation. (a) The thin straight line is the force given by Equ. 1 and 2. The dashed line is the control function given by Equ. 3. The heavy solid line is the combination of the force function and the control function. (b) Two force generators, oriented in opposite directions, combined with a linear elastic shear resistance. With linear elastic resistance, force and shear displacement are proportional, giving a plot that is a phase diagram, showing limit cycle oscillation.

A MODEL FOR NODAL CILIA USING A MATHEMATICAL MODEL FOR FORCE GENERATION AND CONTROL BY SLIDING VELOCITY

This model has been presented in [14]. It starts with a simple mathematical model for a force generator with the property that active shear force decreases with sliding velocity. The model is designed to resemble actual motor enzymes, which produce work by releasing strain. At 0 sliding velocity, active shear force per unit length, $f = F$. F represents the maximum isometric force that can be generated by the currently active population of motors. In response to a sudden shear, the force acts like an elastic element with an elastic constant = $E_{SCB}\,F$. When $f \neq F$, the force recovers towards F with a first-order rate constant, k_1. The model is described by a simple differential equation for f as a function of sliding velocity $\dot{\alpha}$ [16]:

$$\frac{df}{dt} = -E_{SCB}F\dot{\alpha} + k_1(F - f). \tag{1}$$

The steady-state solution (constant sliding velocity) is

$$f = F(1 - E_{SCB}\dot{\alpha}/k_1), \tag{2}$$

giving a linear decrease in force with sliding velocity, with a "maximum" sliding velocity at $\dot{\alpha} = k_1/E_{SCB}$. To create an self-oscillatory system, this force generator is combined with a control function that controls F by sliding velocity:

$$\frac{dF}{dt} = k_2\left(\frac{F_0}{1 + k_3/\dot{\alpha}} - F\right) \qquad \text{for } \dot{\alpha} > 0$$

$$\frac{dF}{dt} = -k_2 F \qquad \text{for } \dot{\alpha} <= 0. \tag{3}$$

where F_0 is the maximum isometric force that can be produced when all of the motors are fully activated, and k_3 is a constant equal to the sliding velocity at which $F = 0.5$ F_0. The time delay process constant k_2 determines how rapidly F follows changes in $\dot{\alpha}$. Figure 2a illustrates the steady state force given by Equ. (1) with constant F, and the control function given by Equ. (3) with very large k_2. Under steady state conditions, the combination of Equations (1) and (3) gives the heavy curve shown in Fig. 2a with the force rising from 0 at $\dot{\alpha}$<= 0 to a maximum and then decreasing to 0 at a velocity close to the maximum sliding velocity = $k_1 l/E_{SCB}$.

The steady state behavior shown in Fig. 2 is not used for modelling, and is only a rough guide to understanding the behavior of this system. Instead, Equ. (1) is integrated to obtain f at the end of a time interval that is assumed to be short enough so that $\dot{\alpha}$ and F on the right hand side of Equ. (1) can be assumed to be constant during the time interval [16]. Two of these force generators operating in opposite directions, in combination with a linear elastic shear resistance, create an oscillator, described by the phase diagram in Fig. 2b [26]. The interpretation of these specifications is that when dyneins on some doublets are producing sliding in one direction, these dyneins remain active as long as the sliding velocity is greater than the velocity at the peak force. If there is an elastic resistance, the force will gradually increase, the velocity will slow down, and once it falls below the velocity for peak force, the active dyneins are shut off, the velocity reverses, and the antagonistic set of dyneins becomes active.

Numerical integration of this system is feasible by separation of time scales, with the linear elastic terms resulting from E_{SCB} and elastic load treated implicitly, and other terms treated explicitly [16]. Non-linear elastic shear resistance, appropriate for elastic interdoublet linkages, is calculated as proposed by Hines and Blum [19]:

$$m_S = E_S\sigma\left(1 - \frac{1}{\sqrt{1 + 0.75\sigma^2}}\right), \tag{4}$$

where m_S represents shear moment per unit length and σ represents shear, in angular units (rad).

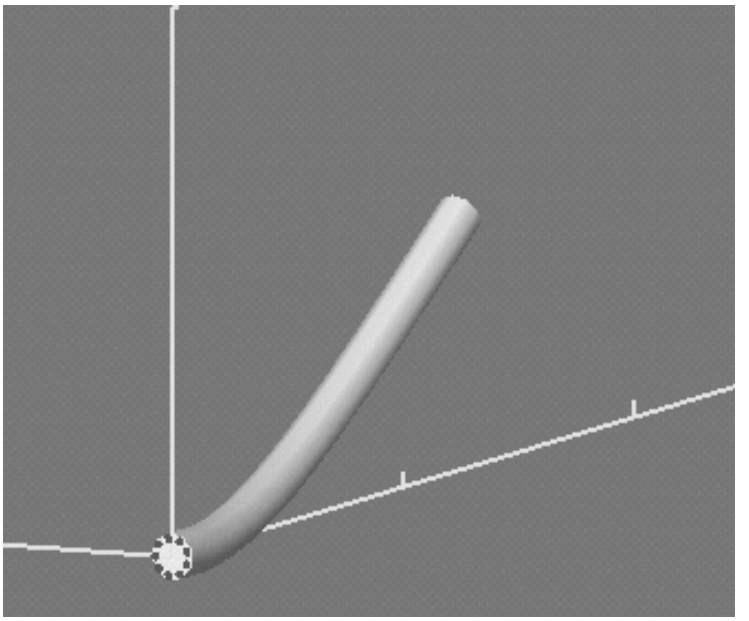

FIGURE 3. One position of a model nodal cilium that is clamped at the basal end and generating a counterclockwise circling motion. Ticks on the Z axis are at 2 μm intervals, and the vertical, Y axis is 2 μm tall. Length of the model is 2.6 μm, circling frequency approx. 10/sec. Parameters used for this computation are the same as for the model in Fig. 2d of [14], except for $E_B = 1.5 \times 10^8$ pN nm^2 and the elastic constant for non-linear shear elasticity is E_S = 44 pN (Equ. 4). Computed with 13 length segments and 0.1 ms time steps.

A model of a nodal cilium, with this force generator distributed along each doublet and a large value of k_2, attempts to oscillate with planar bending, but the bending plane wanders around apparently at random. A stable three-dimensional circling movement is obtained with lower values of k_2 (Fig. 3). To produce this circling movement, force generation must propagate from doublet to doublet around the circumference of the model. No mechanism for circumferential propagation has been programmed into the model. The circumferential propagation is "self-organized" by the mechanical interactions imposed by requiring the force generators on each doublet to reside on the surface of a cylinder [14]. Similar self-organization was observed previously with curvature controlled models for flagella, and termed "doublet metachronism", to emphasize its similarity to metachronal coordination of independent cilia on a surface [13].

What determines the direction of circling by this model? In an earlier study of three-dimensional bending of flagella in which active shear force was controlled by curvature, it was found that the direction of circling could be controlled by the direction of sensitivity to curvature [13]. The same device can be used with the current model, by suggesting that the controlling sliding velocity for dyneins on a particular doublet is measured in a direction that is slightly different than the direction of the sliding produced by those dyneins. While this device is successful [14], it requires, in effect, that dyneins on doublet N are influenced by the sliding velocity on doublet

N+1. A more attractive idea is that dyneins act to rotate or twist their substrate microtubules, resulting in twist of the axoneme. Several examples of clockwise (viewed from base to tip) microtubule rotation by dyneins during in vitro motility assays support this idea [27, 28].

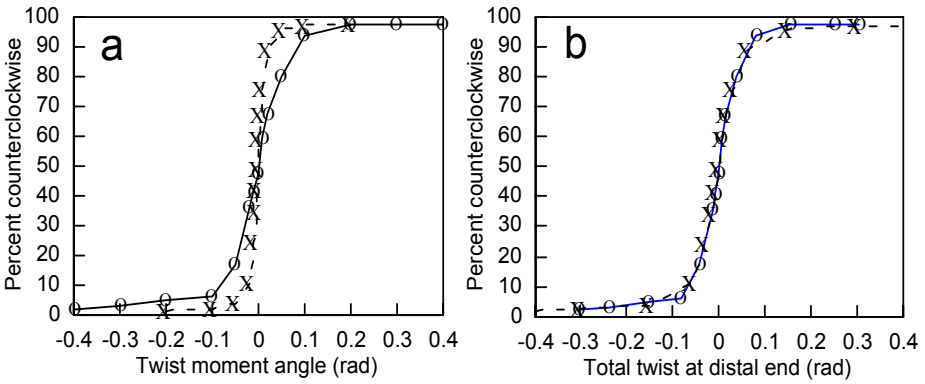

FIGURE 4. Results of computations with a nodal cilium model similar to the model shown in Fig. 3, except that the elastic shear resistance was linear, with E_S = 4 pN. The percentage of counterclockwise circling was determined from 400 computations for each point shown. Points on the solid line, from [14], were obtained with the standard twist resistance, and points on the dashed line were obtained with 25% of that twist resistance.

The effect of off-axis force, which produces a moment that twists the axoneme, is shown in Fig. 4. An off-axis force in the direction that would cause clockwise rotation produces clockwise twist of the axoneme, and results in predominantly counterclockwise circling. Results in Fig. 4 are shown for two series of computations, using two different values of axonemal twist resistance. In Fig. 4a, the results are plotted against the angle of the off-axis force, and in Fig. 4b, the results are plotted against the resulting twist measured at the end of the ciliary model. In the latter case, the curves are superimposed, indicating that it is the actual twist that regulates the circling direction of this model. To obtain this result, it was necessary for the model to include a significant amount of elastic shear resistance, as well as the elastic bend resistance [14].

Once a circling direction is established, the symmetry-breaking twisting moment can be removed or reversed, without any change in circling direction [14]. Computations designed to examine the initial determination of circling direction reveal interesting complexity in the behavior of this dynamic system. An example with one particular set of parameters is shown in Fig. 5. This model uses the non-linear elastic shear resistance of Equ. (4), which is designed to replicate the behavior of elastic linkages between the outer doublets. Maintaining the twist for a time equivalent to half the circling time, or 0.05 sec, is sufficient to obtain results equivalent to maintaining twist throughout the computation, as in Fig. 4. These results are shown along the top edge of the plot in Fig. 5. Along the bottom edge, with no twist, and along the vertical line for 0 twist moment, the results are random, with approximately 50% counterclockwise circling. When the twist is maintained for 0.2 to 0.25 sec, the

response to the higher values of twist is reversed. This can probably be explained if the amount of sliding at times less than 0.25 sec is not sufficient for the non-linear elastic shear resistance to become important. Under this condition, the model then behaves in the same manner as models without elastic shear resistance, with a reversed and weaker effect of twist on circling direction [14]. With intermediate values of twist moment angle and cutoff time, there are other regions of the plot that show unexpected and unexplained behavior. Whether these complexities of behavior have any relevance to the real biological systems remains to be established.

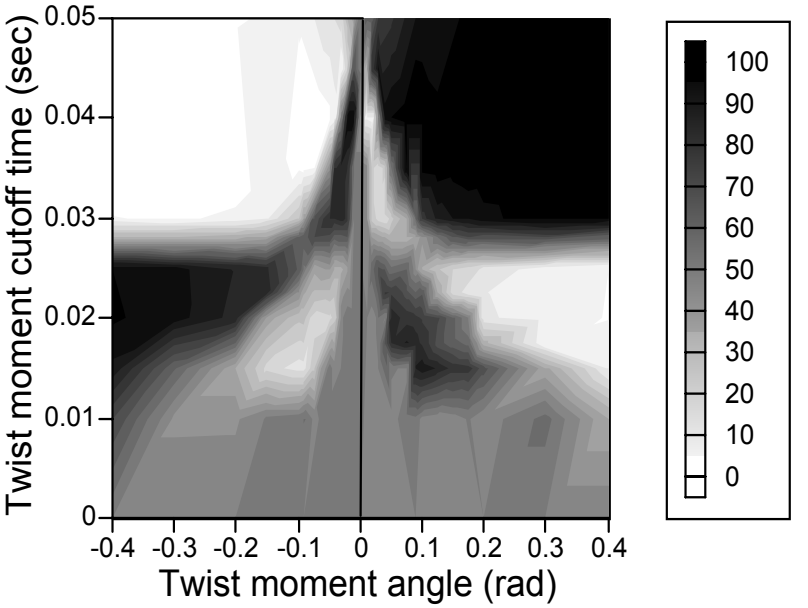

FIGURE 5. Results of computations with the nodal cilium model shown in Fig. 3. The intensity scale represents the percentage of counterclockwise circling, determined from 400 computations at each of 229 pairs of values of twist moment angle and twist moment cutoff time.

EXTENSION TO MODELS WITH STOCHASTIC DYNEINS

A nodal cilium probably contains of the order of 1000 to 3000 dynein motors. If each of these dyneins behaves as an independent force generator, stochastic fluctuations in active shear force will be significant, and the behavior of the model might be expected to be very different from the deterministic model discussed in the previous section. Using stochastic computation of the individual dyneins, the present models can produce circling movements, but the direction of circling is not stable unless additional averaging processes are introduced. These models are not yet adequate for satisfactory examination of symmetry breaking in nodal cilia.

Models that more successfully replicate the movements of real nodal cilia may require consideration of models for dynein motor function that do not assume that

each dynein operates independently of its neighbors. Alternatively, oscillation may result from some form of control mechanism that is much less sensitive to stochastic fluctuations in force and sliding caused by independent operation of individual dyneins. Models in which oscillation results from regulation of dynein activity by sliding velocity are designed to have an instability that leads to oscillation. This may be a good design for a deterministic system, but not for a stochastic system. Despite intensive investigation for more than 50 years, the mechanism for oscillation of cilia and flagella remains a mystery.

REFERENCES

1. McManus, C., *Right Hand, Left Hand*, Cambridge: Harvard University Press, 2002.
2. Berdon, W. E., and Willi, U., *Pediatr. Radiol*. **34**, 38-42 (2004).
3. Hummel, K. P., and Chapman, D. B., *J. Hered*. **50**, 9-13 (1959).
4. Supp, D. M., Witte, D. P., Potter, S. S., and Brueckner, M., *Nature* **389**, 963-966 (1997).
5. Supp, D. M.,Brueckner, M., Kuehn, M. R., Witte, D. P., Lowe, L. A., McGrath, J., Corrales, J., and Potter, S. S. *Development* **126**, 5495-5504 (1999).
6. Nonaka, S., Tanaka, Y., Okada, Y., Takeda, S., Harada, A., Kanai, Y., Kido, M., and Hirokawa, N., *Cell* **95**, 829-837 (1998).
7. Okada, Y., Nonaka, S., Tanaka, Y., Sijoh, Y., Hamada, H., and Hirokawa, N., *Molecular Cell* **4**, 459-468 (1999).
8. Nonaka, S., Shiratori, H., Saijoh, Y., and Hamada, H., *Nature* **418**, 96-99 (2002).
9. Blake, J., and Sleigh, M. A., *Biol. Revs*. **49**, 85-125 (1974).
10. Cartwright, J. H. E., Piro, O., and Tuval, I., *Proc. Natl. Acad. Sci.. USA* **101**, 7234-7239 (2004).
11. Bonnafe, E., Touka, M., AitLounis, A., Baas, D., Barras, E., Ucla, C., Moreau, A., Flamant, F., Dubruille, R., Couble, P., Collignon, J., Durand, B., and Reith, W., *Mol. Cell. Biol*. **24**, 4417-4427 (2004).
12. Summers, K. E., and Gibbons, I. R., *Proc. Natl. Acad. Sci. USA*, **68**, 3092-3096 (1971).
13. Brokaw, C. J., *Cell Motil. Cytoskel*. **53**, 103-124 (2002).
14. Brokaw, C. J. *Cell Motil. Cytoskel*. **60**, 35-47 (2005).
15. Omoto, C. K., and Brokaw, C. J., *J. Cell Sci*. **58**, 385-409 (1982).
16. Brokaw, C. J., *Biophys. J.* **48**, 633-642 (1985).
17. Brokaw, C. J., *Biophys. J.* **12**, 564-586 (1972).
18. Brokaw, C. J., *Cell Mot. Cytoskel.* **28**, 199-204 (1994).
19. Hines, M., Blum, J. J., *Biophys. J.* **23**, 41-57 (1978).
20. Lindemann, C. B., *Cell Mot. Cytoskel*. **29**, 141-154 (1994).
21. Huxley, A. F., *Prog. Biophys*. **7**, 255-318 (1957).
22. Burgess, S. A., Walker, M. L., Sakakibara, H., Knight, P. J., and Oiwa, K., *Nature.* **421**, 715-718 (2003).
23. Brokaw, C. J., *Biophys. J.* **73**, 938-951 (1997).
24. Kon, T., Nishiura, M., Ohkura, R., Toyoshima, Y. Y., and Sutoh, K., *Biochemistry.* **43**, 11266-11274 (2004).
25. Brokaw, C. J., *Biophys. J.* **16**, 1013-1027 (1976).
26. Brokaw, C. J., *Proc. Natl. Acad. Sci.. USA* **72**, 3102-3106 (1975).
27. Vale, R. D., and Toyoshima, Y. Y., *Cell.* **52**, 459-469 (1988)
28. Kagami, O., and Kamiya, R., *J. Cell Sci.* **103**, 653-664 (1992).